# COUPLING MEASUREMENTS IN ATF2 EXTRACTION LINE

C. Rimbault, P. Bambade, LAL, Univ Paris-Sud, IN2P3/CNRS, Orsay, France
S. Kuroda, T.Tauchi, N.Terunuma, KEK, Japan
G. White, M. Woodley, SLAC, Stanford, USA

*Abstract*

The purpose of ATF2 is to deliver a beam with stable very small spotsizes as required for future linear colliders such as ILC or CLIC. To achieve that, precise controls of aberrations such as dispersion and coupling are necessary. Theoretically, the complete reconstruction of the beam matrix is possible from the measurements of horizontal, vertical and tilted beam sizes, combining skew quadrupole scans at several wire-scanner positions. Such measurements were performed in the extraction line (EXT) of ATF2 in May 2009. We present analysis results attempting to resolve the $4 \times 4$ beam matrix.

## INTRODUCTION

The commissioning of ATF2, the final focus line of ATF installed at the exit of the ATF redesigned extraction line (EXT), started at the end of 2008. To deliver a stable beam of 37 nm vertical size at the interaction point, most of the aberrations such as coupling must be corrected at the upstream of the final focus line, in the EXT. Since 1998 several studies have underlined that the vertical emittance measured in the EXT is much larger (about a factor three) than the one measured in the damping ring (DR) [1]. Recent studies [2] demonstrated a large coupling of the beam in the EXT which can arise from several sources, such as the DR, some shared magnets between the DR and the EXT, the skew quadrupoles used for dispersion correction, etc... Coupling is corrected with 4 skew quadrupoles installed in the dispersion free region of EXT. The knowledge of the four coupling beam matrix elements would enable the correction required by each skew quad to be directly calculated. We first briefly review the basic formalism of beam optics and explain how theoretically it is possible to obtain a complete resolution of the coupling components of a beam [3]. We then present the results of the coupling measurements performed during ATF2 commissioning and the results of the analysis aiming to determine the complete beam matrix.

## BASIC FORMALISM

The evolution of a beam matrix:

$$\sigma = \begin{pmatrix} \sigma_{11} & \sigma_{12} & \sigma_{13} & \sigma_{14} \\ \sigma_{12} & \sigma_{22} & \sigma_{23} & \sigma_{24} \\ \sigma_{13} & \sigma_{23} & \sigma_{33} & \sigma_{34} \\ \sigma_{14} & \sigma_{24} & \sigma_{34} & \sigma_{44} \end{pmatrix}$$

between two points, A and B, of an uncoupled transfer line is described by the following matrix equation:

$$\sigma^B = R\sigma^A R^T \ , \tag{1}$$

where R is the linear transfer matrix between the two points. The elements $\sigma_{13} =< xy >$, $\sigma_{14} =< xy' >$, $\sigma_{23} =< x'y >$ and $\sigma_{24} =< x'y' >$ represent the coupling terms which have to be as small as possible for a high quality beam. Experimentally, only $\sigma_{11} =< xx >= \sigma_x^2$ and $\sigma_{33} =< yy >= \sigma_y^2$ are directly measurable from horizontal and vertical beam size measurements. One can also deduce $\sigma_{13} =< xy >$ by measuring the beam size,$\sigma_{phi}$, along a tilted axis at an angle $\phi$ with respect to the x-axis, from the equation [4, 5]:

$$\sigma_{13} = \frac{\sigma_\phi^2}{2\cos\phi\sin\phi} - \frac{\sigma_x^2\cos\phi}{2\sin\phi} - \frac{\sigma_y^2\sin\phi}{2\cos\phi}$$

From these measurements one can theoretically reconstruct all of the beam matrix elements, using skew quadrupole scans. Developping Equation (1) and using the thin lens approximation for the skew quad transfer matrix, the following expressions for the measurable beam elements are obtained:

$$\sigma_{11}^M = k^2 R_{12}^2 \sigma_{33}^Q \tag{2}$$
$$+ 2k(R_{11}R_{12}\sigma_{13}^Q + R_{12}^2\sigma_{23}^Q) \tag{3}$$
$$+ R_{11}^2\sigma_{11}^Q + 2R_{11}R_{12}\sigma_{12}^Q + R_{12}^2\sigma_{22}^Q \tag{4}$$

$$\sigma_{33}^M = k^2 R_{34}^2 \sigma_{11}^Q \tag{5}$$
$$+ 2k(R_{33}R_{34}\sigma_{13}^Q + R_{34}^2\sigma_{14}^Q) \tag{6}$$
$$+ R_{33}^2\sigma_{33}^Q + 2R_{33}R_{34}\sigma_{34}^Q + R_{34}^2\sigma_{44}^Q \tag{7}$$

$$\sigma_{13}^M = k^2 R_{12}R_{34}\sigma_{13}^Q \tag{8}$$
$$+ k[R_{11}R_{34}\sigma_{11}^Q + R_{12}R_{33}\sigma_{33}^Q + R_{12}R_{34}(\sigma_{12}^Q + \sigma_{34}^Q)] \tag{9}$$
$$+ R_{11}R_{33}\sigma_{13}^Q + R_{11}R_{34}\sigma_{14}^Q + R_{12}R_{33}\sigma_{23}^Q + R_{12}R_{34}\sigma_{24}^Q \tag{10}$$

The measured elements, $\sigma_{11}^M$, $\sigma_{33}^M$ and $\sigma_{13}^M$, can be expressed as parabolic functions, $\sigma^2 = A(k-B)^2 + C$, of the skew quadrupole strength, $k$, described by the 3 fit parameters $A$, $B$ and $C$. The sub-equations (2), (5) and (8) are relative to the parameter $A$, the sub-equations (3), (6) and (9) are relative to the product $AB$ and the sub-equations (4), (7) and (10) are relative to the combination $AB^2 - C$.

## COUPLING MEASUREMENTS

We based our analysis on three sets of beam size measurements at four wire-scanner positions, MW1X, MW2X, MW3X and MW4X for several strengths of the first skew quadrupole, QK1X. In addition to the horizontal and vertical projected beam sizes, the projected beam size at two different tilted axis, $80^o$ and $100^o$ from the horizontal axis, have been measured. We thus obtained two ways to reconstruct $\sigma_{13}$, and consequently to verify the coherence of the measurements at $80^o$ and $100^o$. This is shown on Figure 1, where one can see the good agreement between the two measurements. The large errors were dominated by the $\sigma_\phi$ measurement errors inherent to the previous data acquisition system, which is now upgraded.

We have also verified the physical meaning of the beam ellipse for each measurement as displayed on figure 2, using the fact that, from $\sigma_x$, $\sigma_y$ and $\sigma_\phi$, one can calculate the major axis, $a = \sqrt{\frac{1}{2}(\sigma_x^2 + \sigma_y^2 + \frac{\sigma_x^2 - \sigma_y^2}{\cos 2\theta})}$, the minor axis, $b = \sqrt{\frac{1}{2}(\sigma_x^2 + \sigma_y^2 - \frac{\sigma_x^2 - \sigma_y^2}{\cos 2\theta})}$, as well as the tilted angle, $\theta$, of the beam ellipse for which $\tan 2\theta = \frac{2\sigma_\phi^2 - \sigma_x^2 - \sigma_y^2}{(\sigma_x^2 - \sigma_y^2)\sin 2\phi} - \frac{\cos 2\phi}{\sin 2\phi}$

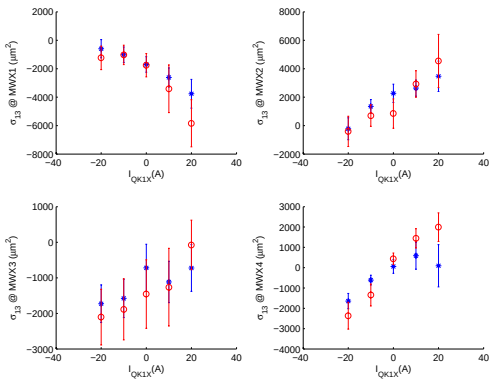


Figure 1: Reconstruction of $\sigma_{13}$ from the beam size measurements at $80^o$ in blue and at $100^o$ in red.

## BEAM MATRIX RECONSTRUCTION

For the complete beam matrix reconstruction we used both the skew quad scan method and the multi-wire position one both discribed in ref. [2]. Indeed, skew quad scans at one location is not enough to solve all the elements since this represents a system of only nine equations for ten parameters. Moreover, the horizontal beam size parabola is most of the time hard to fit because of its flatness. The fits of $\sigma_{33}$ and $\sigma_{13}$ are displayed on Figure 3. To reconstruct the beam matrix, the most straight forward way is to consider a simplified system, only composed of the sub-equations 4, 7 and 10, at the four wire scanner locations.In this system, the resolution of the coupling elements are mainly independant of the resolution the $2 \times 2$ diagonal ones. We used the direct multi-wire method for the beam sizes at k=0 on one hand (method 1), and the combinations of the fitted parameters from parabolas at the four locations on the other hand (method 2). These two methods are of course not strictly independant, but the latter is hoped to be more accurate. The beam matrix elements reconstructed at QK1X by these two methods are in the first part of the table . Both methods lead to the same coupling reconstruction, but unphysical since the correlations are about two orders of magnitude larger than one!

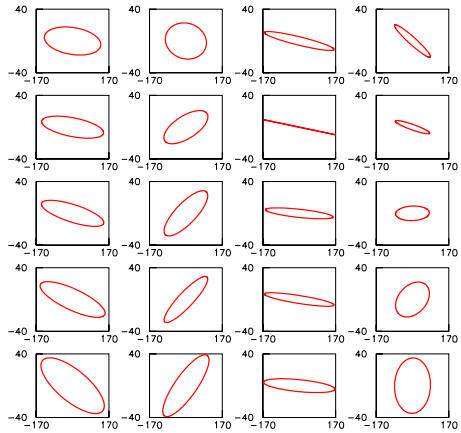

Figure 2: Reconstructed beam ellipses at each wire scanner (from the left to the right) and for each strength of the skew quad we fixed (from the top to the down).

Another way (method 3) is to first consider the four good fits of $\sigma_{33}$ (fig.003) at from which one can deduce six of ten beam matrix elements, $\sigma_{11}^Q$, $\sigma_{13}^Q$, $\sigma_{14}^Q$, $\sigma_{33}^Q$, $\sigma_{34}^Q$ and $\sigma_{44}^Q$. Then, using the previously determined elements, one uses the four fits of $\sigma_{13}$ to reconstruct $\sigma_{12}^Q$, $\sigma_{23}^Q$, and $\sigma_{24}^Q$. Finally the $\sigma_{11}$ fits will constrain only $\sigma_{22}$. The results of this reconstruction method are displayed in the second part of the table . Coupling elements are then much smaller than with the previous methods, and lead to a physical beam matrix. Horizontal and vertical emittances are respectively $(2.5 \pm 0.2)$ nm.rad and $(31 \pm 15)$ pm.rad.

We then compare our measurements with the results of the propagation of the reconstructed beam matrix from QK1X to each wire-scanner locations. Figures 4 and 5 show the comparison between the measurements in red and the analysis results in blue respectively for the vertical and $< xy >$ beam sizes. Except MW3X $\sigma_{33}$ measurements are very well reproduced by the reconstructed matrix. $\sigma_{13}$ is dominated by very large errors, to conclude on the coherence of the results with the measurements for MW1X, MW2X and MW3X would be tantalising but too much optimistic. It seems $\sigma_{13}$ measurements lead to larger estimate of coupling than is be expected. This probably arises from uncertainties in the measurement of the wire tilts.

## CONCLUSIONS

We aimed to reconstruct the full beam matrix using only skew quadrupole scans at different EXT wire-scanner locations, with measurements of horizontal, vertical and two

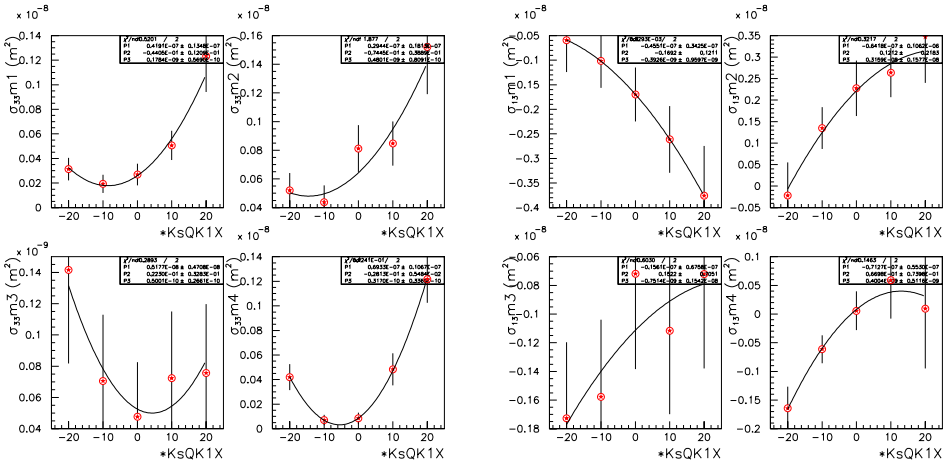


Figure 3: $\sigma_{33}$ on l.h.s and $\sigma_{13}$ on r.h.s measurements as a function of the strength of the skew quad, at MW1X, MW2X, MW3X and MW4X.

Table 1: Reconstructed beam matrix elements at QK1X with the three methods described in the text.

| | $\sigma^Q_{11}$ | $\sigma^Q_{12}$ | $\sigma^Q_{22}$ | $\sigma^Q_{33}$ | $\sigma^Q_{34}$ | $\sigma^Q_{44}$ | $\sigma^Q_{13}$ | $\sigma^Q_{14}$ | $\sigma^Q_{23}$ | $\sigma^Q_{24}$ |
|---|---|---|---|---|---|---|---|---|---|---|
| method 1 | 2.8e-9 | -2.5e-9 | 3e-9 | 1.6e-10 | 5.6e-11 | 2.1e-11 | 1.7e-7 | 3.4e-8 | 7.5e-9 | 6.6e-8 |
| method 2 | 9.9e-9 | -2.4e-9 | -5.4e-10 | 8.2e-11 | 2.0e-11 | 1.7e-11 | 1.7e-7 | 3.4e-8 | 7.5e-9 | 6.7e-8 |
| method 3 | 3.6e-9 | -2.1e-9 | 2.9e-9 | 8.2e-11 | 2.0e-11 | 1.7e-11 | -6.8e-11 | 1.6e-10 | 1.8e-10 | 4.1e-11 |

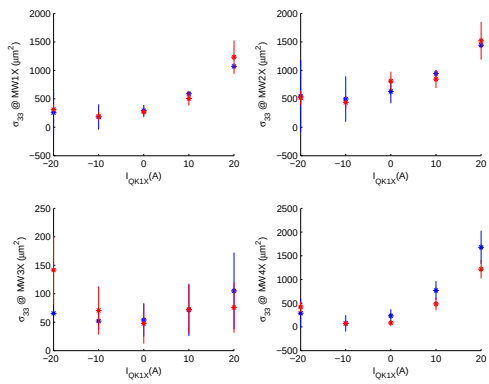


Figure 4: $\sigma_{33}$, from beam matrix reconstruction in blue and from measurements in red, as a function of the strength of the skew quad, at MW1X, MW2X, MW3X and MW4X.

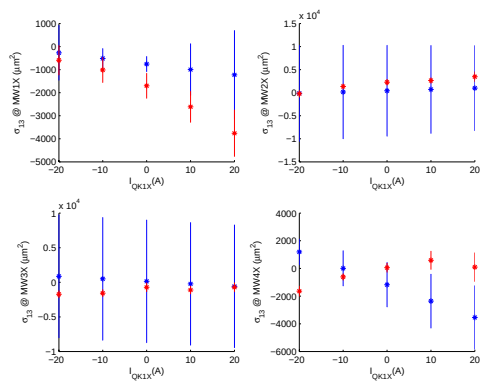


Figure 5: $\sigma_{13}$, from beam matrix reconstruction in blue and from measurements in red, as a function of the strength of the skew quad, at MW1X, MW2X, MW3X and MW4X.

tilted beam size projections. Checking the coherence of the $\sigma_{13}$ reconstruction from the $\sigma_{80^\circ}$ and the $\sigma_{100^\circ}$ measurements was essential to perform this analysis. We have shown that reconstruction of the coupling element can not be performed independantly of the $4 \times 4$ diagonal ones since it leads to unphysical results. A more accurate and automatisable method was find, leading to physical beam matrix reconstruction, compatible with the measurements. Another analysis should be performed based on a larger number of data sets to minimise statistical errors.

## REFERENCES

[1] J. Turner, M. Woodley, H. Hayano, ATF INTERNAL REPORT ATF-99-17, (1999).

[2] C. Rimbault et al., EPAC08-TUPC087, (2008).

[3] M. R. Rees, L. Rivkin SLAC-PUB-3305, SLAC/AP-18, (1984).

[4] I. Agapov, G. A. Blair, M. Woodley, Phys. Rev. ST Accel. Beams 10, 112801 (2007).

[5] P. Emma, M. Woodley, ATF-99-04, (1999).